



Universiteit
Leiden
The Netherlands

Host-directed therapy for intracellular bacterial Infections

Korbee, C.J.

Citation

Korbee, C. J. (2019, March 6). *Host-directed therapy for intracellular bacterial Infections*. Retrieved from <https://hdl.handle.net/1887/69481>

Version: Not Applicable (or Unknown)

License: [Licence agreement concerning inclusion of doctoral thesis in the Institutional Repository of the University of Leiden](#)

Downloaded from: <https://hdl.handle.net/1887/69481>

Note: To cite this publication please use the final published version (if applicable).

Cover Page



Universiteit Leiden



The handle <http://hdl.handle.net/1887/69481> holds various files of this Leiden University dissertation.

Author: Korbee, C.J.

Title: Host-directed therapy for intracellular bacterial Infections

Issue Date: 2019-03-06

2 | A Novel Medium-Throughput siRNA and Chemical Compound Screening Assay for Host Regulation of Intracellular Bacterial Infections

Cornelis J. Korbee, Elisabeth van Strijen, Kees L. M. C. Franken, Louis Wilson, Nigel D. L. Savage, Mariëlle C. Haks**, Tom H. M. Ottenhoff**

Bacterial drug-resistance poses severe global health problems. Recent efforts to identify novel antibiotics yielded only a limited number of leads, prompting for novel approaches, including host-directed therapies. Intracellular pathogens like *Salmonellae* (*Stm*) and *Mycobacterium tuberculosis* (*Mtb*) manipulate host signaling networks to promote their survival but knowledge of the precise molecular interactions at the pathogen-host interface is limited. Chemical and genetic perturbation of host cell signaling and inflammation has been shown to inhibit growth of intracellular pathogens, but relatively few host targets or chemical compounds have been identified so far. To accelerate target identification, we have developed and validated a medium-throughput flow cytometry-based screening assay, employing highly manipulable, *Stm*- as well as *Mtb*-infectable human cell-lines, combined with (novel) (myco)bacterial fluorescent protein constructs. The assay is fast, highly reproducible, concurs with classical bacterial growth inhibition assays, provides an excellent screening window, is applicable to both siRNA and chemical compound screens and validates well in human primary macrophages.

Adapted from:

Korbee, C.J.*, Heemskerk, M.T.*, Kocev, D., van Strijen, E., Rabiee, O., Franken, K.L.M.C., Wilson, L., Savage, N.D.L., Džeroski, S., Haks, M.C.**; Ottenhoff, T.H.M.**; 2018. **Combined chemical genetics and data-driven bioinformatics approach identifies receptor tyrosine kinase inhibitors as host-directed antimicrobials.** *Nat Commun* **9**, 358. doi:10.1038/s41467-017-02777-6.

* Contributed equally

** Contributed equally

Introduction

Bacterial antibiotic resistance is a widespread and increasing problem in modern medicine. Although a number of novel candidate antibiotics have recently been identified¹, current antibiotics already cover the majority of druggable targets of pathogens, resulting in a continuous decline in the number of newly discovered and approved antibiotics²⁻⁷. Intracellular bacteria present additional challenges as they are often able to manipulate host cell signaling to induce a survival niche and thereby subvert both innate and adaptive immunity. Knowledge of the mechanisms involved, however, also creates new opportunities for treatment, for instance by pharmacological perturbation of host cell signaling or inflammation to induce killing of intracellular bacteria and to promote effective host defense⁸. Here, we focused on the major human pathogens *Salmonella enterica* and *Mycobacterium tuberculosis* (*Mtb*). *Salmonella enterica* serovar Typhimurium (*Stm*) is a common causative agent of gastroenteritis in humans and causes a systemic disease resembling human typhoid fever in a murine host⁹. Following ingestion by the host, the bacterium induces its uptake by otherwise non-phagocytic intestinal epithelial cells. This is mediated by Salmonella Pathogenicity Island 1 (SPI1) encoded effectors, which translocate to the host cytoplasm through a Type III Secretion System (T3SS). The effectors then induce actin cytoskeleton remodeling and the subsequent formation of the Salmonella-Containing Vesicle (SCV)¹⁰. The SCV interacts with both early and late endosomes, is relatively acidic and acquires lysosomal markers like LAMP-1^{11,12}. *Mtb* is a facultative intracellular pathogen, which upon entry in the lung is phagocytosed by alveolar Mφs¹³. By modulating the host cell microbicidal machinery *Mtb* establishes an intracellular niche in which it can survive and replicate¹⁴. The subsequent induction of granuloma formation enables *Mtb* to persist within the human host for decades¹⁵. With an estimated one fourth of the world population carrying a latent *Mtb* infection and a resulting 1.8 million annual deaths, TB remains a critical global health problem¹⁶⁻²⁰.

Several recent studies, including our own, have demonstrated the feasibility of host-directed approaches to combat bacterial drug-resistance both *in vitro*²¹⁻²⁵ and *in vivo*²⁶⁻³⁶. Using reciprocal chemical genetics focusing on systematic perturbation of the host cell kinome we identified AKT1 as a central regulator of *Stm* intracellular survival in human cells. Treatment of infected cells with H-89, a chemical inhibitor of AKT1, decreased the *Stm* bacterial load and this bacterial growth inhibition by H-89 was reproduced in *Mtb* infected human macrophages (Mφs)²¹. However, HDT approaches have not yet led to clinically applicable drugs and additional chemical compounds for HDT and more detailed fundamental understanding of molecular host-pathogen interactions are needed for development of HDT strategies into feasible clinical applications.

There are several major challenges to be overcome to facilitate host-directed chemical-genetic studies targeting intracellular pathogens, particularly studies that aim at discovering key host pathways manipulated by *Mtb*. Firstly, it is extremely difficult to generate sufficient quantities of primary Macrophages (Mφs), the natural target cells for *Mtb* infection, from human donors for medium-throughput screens, even by pheresis. Secondly, the often-used THP-1 monocytic

cell line requires PMA stimulation for differentiation, which massively affects cell signaling and vesicular trafficking^{37,38}, thus confounding cellular signaling studies. Thirdly, there is a lack of fast (compared to the classical 3-week *Mtb* Colony Forming Unit (CFU) assay), robust and widely applicable readouts for rapid screening. Finally, achieving stable genetic knockdown in human primary Mφs is challenging, especially in large siRNA screens where knockdown efficiency of each individual gene cannot broadly be confirmed. To solve these problems, we have developed a rapid, medium-throughput, fluorescence-based screening assay to determine bacterial load by automated flow cytometry in the highly manipulable human HeLa and MelJuSo cell lines infected with (myco)bacteria expressing novel (myco)bacterial fluorescent protein constructs. Our identification of the MelJuSo cell line as a novel *Mtb* infection model has several important advantages: MelJuSo cells are suited to large scale screening assays as they are more homogenous than primary cells, do not require additional stimuli like PMA for maturation, can be efficiently manipulated using RNAi, and can be infected by mycobacteria³⁹. We have shown in the past that human melanocytes can efficiently present mycobacterial antigens to HLA class II restricted CD4 T cells⁴⁰ and have successfully used MelJuSo to dissect molecular pathways of MHC class II presentation in human cells^{41,42}. Our novel fluorescence-based bacterial growth assay is applicable for both siRNA and chemical compound screens, and is equally suitable for both *Stm* and *Mtb* despite the vast differences in their intracellular 'lifestyles' and replication rates (20 minutes and 18 hours, respectively)^{8,9,13,14}, demonstrating the versatility of this assay.

Results

A flow cytometry-based readout for intracellular bacterial load.

To uncover host pathways controlling intracellular bacterial survival, we developed a fast, robust and novel assay suitable for medium-throughput (96-well) compound and siRNA screening, employing flow cytometry as a readout for intracellular bacterial load using fluorescent strains of *Stm* and *Mtb*. We used the PKB/AKT1 kinase inhibitor H-89 as initial reference compound, since we had identified H89 as an effective HDT with antimicrobial activity against *Mtb* and *Stm* previously²¹. Optimization data for fluorescent reporters expressed in *Stm* and *Mtb* is described below. Importantly, our novel medium-throughput flow cytometry-based assay to screen compound and siRNA libraries allows accurate determination of *Mtb* bacterial load within 24h and 72h, respectively, which greatly shortens the time to readout compared to the classical 3-4 week CFU assay for *Mtb*. HeLa (cervical carcinoma) and MelJuSo (melanoma) human cell lines were selected as host models for *Stm* and *Mtb* infection, respectively. In contrast to non-phagocytic HeLa cells, melanocytes were previously reported to possess phagocytic capacity³⁹, a prerequisite for uptake of mycobacteria. Conversely, MelJuSo was not found to be a suitable target cell line for *Stm* infection as *Stm* did not propagate well in these cells, in line with the previously reported aberrant phenotype of *Stm* in MelJuSo⁴³. As chemical compounds may exhibit auto-

fluorescence and therefore may cause false positive results when detecting increases in bacterial load, the assay for screening chemical compounds is ideally suited for detecting decreases in bacterial loads.

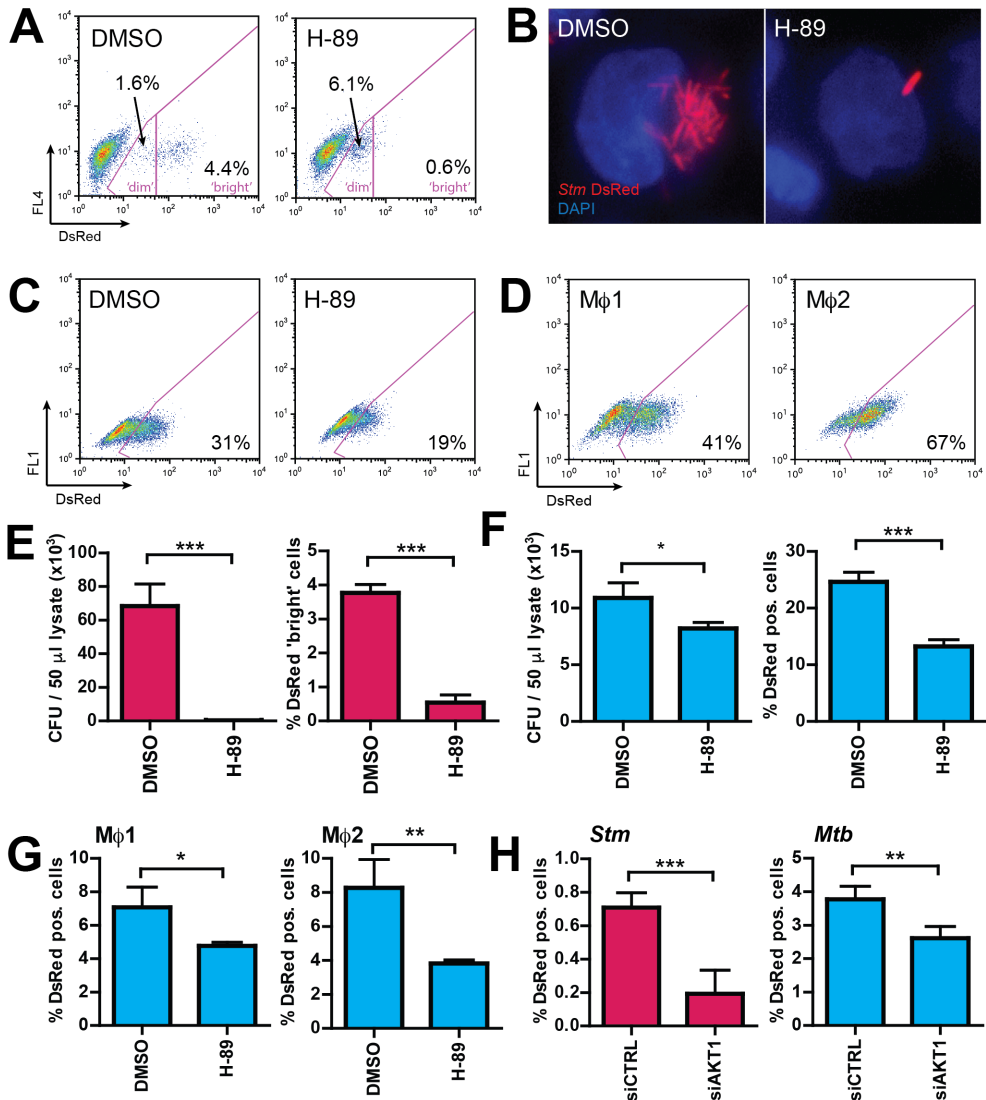
In HeLa cells infected with genetically-tagged DsRed-*Stm* both DsRed 'bright' and 'dim' infected cell populations were observed (**Figure 1A**). H-89 treatment markedly diminished the DsRed 'bright' population. Since H-89 treatment effectively reduced *Stm* bacterial numbers in HeLa cells as measured by CFU (**Figure 1E**)²¹, this DsRed 'bright' population represents cells containing proliferating bacteria. The reduction in *Stm* bacterial load by H-89 treatment was corroborated by fluorescence microscopy (**Figure 1B**). Similarly, *Mtb* infection of MelJuSo cells could be visualized using flow cytometry (**Figure 1C**) and H-89 also decreased the bacterial load in this infection model (**Figure 1F**). Importantly, since alveolar Mφs are the primary target cells for *Mtb in vivo*, we verified that infection of these cells can be similarly visualized using flow cytometry (**Figure 1D**) and that H-89 treatment decreased bacterial loads in primary human pro-inflammatory (Mφ1) as well as anti-inflammatory (Mφ2) cells similar to MelJuSo cells (**Figure 1G**). However, we observed considerable batch-to-batch variation in the proportion of infected Mφs, further supporting the use of the homogenous MelJuSo cell line as an infection model for screening.

We next optimized both the reverse siRNA transfection strategy and bacterial infection conditions by varying cell density, multiplicity of infection (MOI), infection time point and the harvesting time point for analysis using the optimal fluorescent reporters in a medium-throughput setting (outlined below). Using the optimized conditions, knockdown of AKT1 resulted in a significant decrease of both *Stm* and *Mtb* survival in infected cells (**Figure 1H**), but again less so for *Mtb* than for *Stm*, mimicking the effect of treatment of infected cells with AKT1 inhibitor H-89 (**Figures 1E and F**).

In summary, we conclude that HeLa and MelJuSo cells represent new human model systems to study intracellular *Stm* and *Mtb* infection, respectively, providing novel models for medium-throughput screening of host-directed compounds and genetic manipulation to increase our understanding and treatment of intracellular bacterial infections. Importantly, our novel medium-throughput flow cytometry-based assay allows accurate determination of intracellular *Mtb* bacterial load in compound or siRNA treated cells within a significantly shorter time (2-3 days) window than classical CFU assays (3-4 weeks). The assay is suitable for *Stm*, *Mtb* and possibly other intracellular bacterial infection models, despite the vast differences in their intracellular 'lifestyles' and replication rates (20 minutes and 18 hours for *Stm* and *Mtb*, respectively)^{8,9,13,14}.

Optimization of fluorescent reporters for flow cytometry-based quantitation of bacterial infection.

To optimize our assay we explored different fluorescent reporters for expression in *Stm* or *Mtb*. Firstly, we monitored the long-term expression kinetics of GFP and DsRed transcribed from plasmids with an identical backbone in *Mtb* (**Table 1**). Despite hygromycin selection, the *Mtb* culture gradually lost GFP expression over



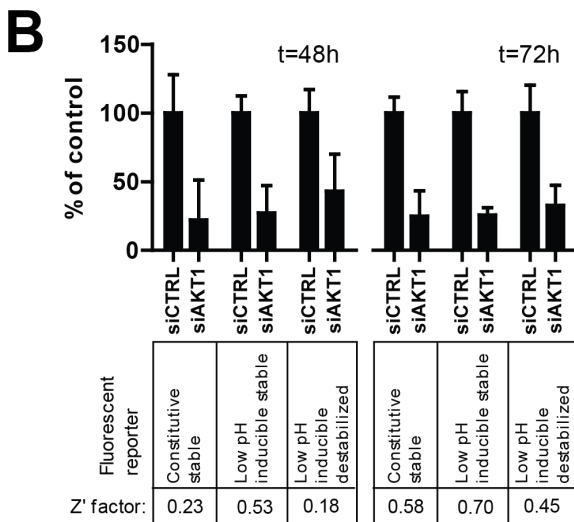
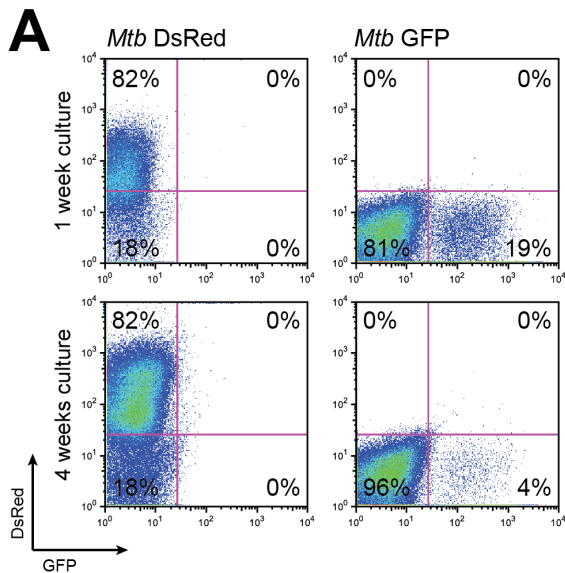
↑ **Figure 1. A flow cytometry-based readout for intracellular bacterial load.**

A. Flow cytometry gating strategy. Shown are dot plots of HeLa cells infected with *Stm* constitutively expressing stable DsRed and treated with H-89 or DMSO at 10 μ M as a negative control. Gates were drawn for separate analysis of total DsRed positive and DsRed 'bright' populations. Percentages of DsRed positive events in each gate are indicated. **B.** Fluorescence microscopy of HeLa cells infected and treated as in **A**. A representative infected cell is shown for both conditions. **C.** Flow cytometry gating strategy for MelJuSo cells infected with *Mtb* constitutively expressing stable DsRed and treated as in **A**. Percentages of DsRed positive events are indicated. **D.** Flow cytometry of human primary Mφ1 (left panel) and Mφ2 (right panel) macrophages infected with *Mtb* constitutively

expressing stable DsRed. Percentages of DsRed positive events are indicated. **E.** Comparison of CFU assay (left panel) to the flow cytometry-based screening assay (right panel) for HeLa cells infected and treated as in **A**. A representative result of 3 experiments is shown. Bars display mean \pm standard deviation. Statistical significance was tested using a t-test. **F.** Comparison of CFU assays (left panel) to the flow cytometry-based screening assay (right panel) is shown for MelJuSo cells infected and treated as in **C**. A representative result of 3 experiments is shown. Bars display mean \pm standard deviation. Statistical significance was tested using a t-test. **G.** Flow cytometry of M ϕ 1 and M ϕ 2 cells infected and treated as in **C**. Bars display mean \pm standard deviation. Statistical significance was tested using a t-test. **H.** Infection of AKT1-silenced HeLa or MelJuSo cells with *Stm* expressing low pH-inducible, stable DsRed (left panel) and *Mtb* constitutively expressing destabilized DsRed (right panel), respectively, analyzed by flow cytometry. Bars display mean \pm standard deviation. Statistical significance was tested using a t-test. Shown are results of 6 replicate samples from 1 representative screening plate out of more than 20 replicate plates. (* = p-value <0.05, ** = p-value <0.01, *** = p-value <0.001).

time, whereas DsRed expression remained unaltered (**Figure 2A**). As loss of fluorescence would be detrimental to a flow-cytometry-based assay, GFP was excluded as a suitable fluorescent reporter in *Mtb*.

As demonstrated in **Figure 1**, constitutively expressed, stable DsRed constructs provided an excellent assay window to reliably evaluate the effect of chemical compound treatment on bacterial loads of both *Stm*- and *Mtb*-infected cells. Compared to compound treatment experiments, quantification of bacterial infection in siRNA transfected cells often resulted in more subtle phenotypes requiring further assay optimization: while the constitutive expression and high stability of fluorescent reporters can negatively impact the sensitivity of fluorescence-based bacterial growth inhibition assays, this can be overcome by employing conditionally expressed or destabilized fluorescent reporters (decreasing the half-life of DsRed from 4.6 days to several hours)^{44,45}. To this end, different fluorescent reporter construct variants (**Table 1**) were expressed in *Stm* (constitutively-expressed stable DsRed, low pH-inducible expressed stable DsRed, or low pH-inducible expressed destabilized DsRed) or in *Mtb* (constitutively-expressed stable DsRed or constitutively-expressed destabilized DsRed) and these bacteria were subsequently used in our HeLa-*Stm* and MelJuSo-*Mtb* infection models following AKT1 silencing. As demonstrated in **Figure 2B**, a low pH-inducible expressed stable DsRed variant increased the assay window in *Stm*-infected HeLa cells following AKT1 silencing ($Z' = 0.70$) compared to constitutively-expressed stable DsRed ($Z' = 0.58$) and low pH-inducible expressed destabilized DsRed ($Z' = 0.45$). The effect of AKT1 silencing in *Mtb*-infected MelJuSo cells could only be visualized using an *Mtb* strain expressing a destabilized DsRed variant (**Figure 1H**), demonstrating that employing this novel fluorescent reporter overcomes a major limitation of fluorescent signal-based growth inhibition assays for slowly replicating bacteria.



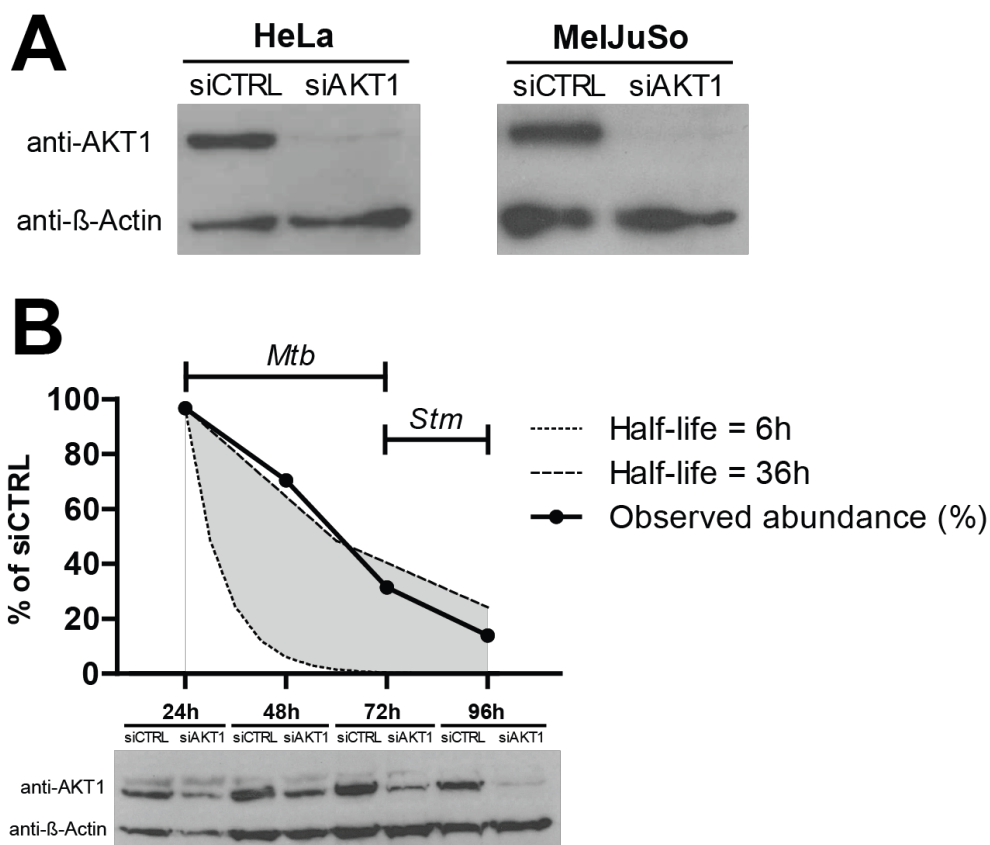
← **Figure 2. Optimization of the flow cytometry-based assay to monitor bacterial load using different fluorescent reporters.**

A. Flow cytometric analysis of DsRed (left panel) and GFP (right panel) expression in *Mtb* cultured for either 1 week (top panel) or 4 weeks (bottom panel) after thawing of a frozen batch. **B.** Infection of HeLa cells using *Stm* strains expressing different fluorescent reporters (constitutive stable, low pH-inducible stable and low pH-inducible destabilized DsRed) at 48 hours (left panel) or 72 hours (right panel) post transfection with the indicated siRNA oligos. siCTRL: scrambled siRNA. The upper panel gives the level of inhibition of intracellular *Stm* in siAKT1 silenced cells expressed as a percentage of the control (siCTRL treated) condition \pm standard deviation. The signal window resulting from infection with the indicated fluorescent *Stm* strains is expressed as a Z' factor.

HeLa-*Stm* and MelJuSo-*Mtb* infection models combined with a flow cytometry-based readout for intracellular bacterial load allow medium-throughput screening of siRNA libraries.

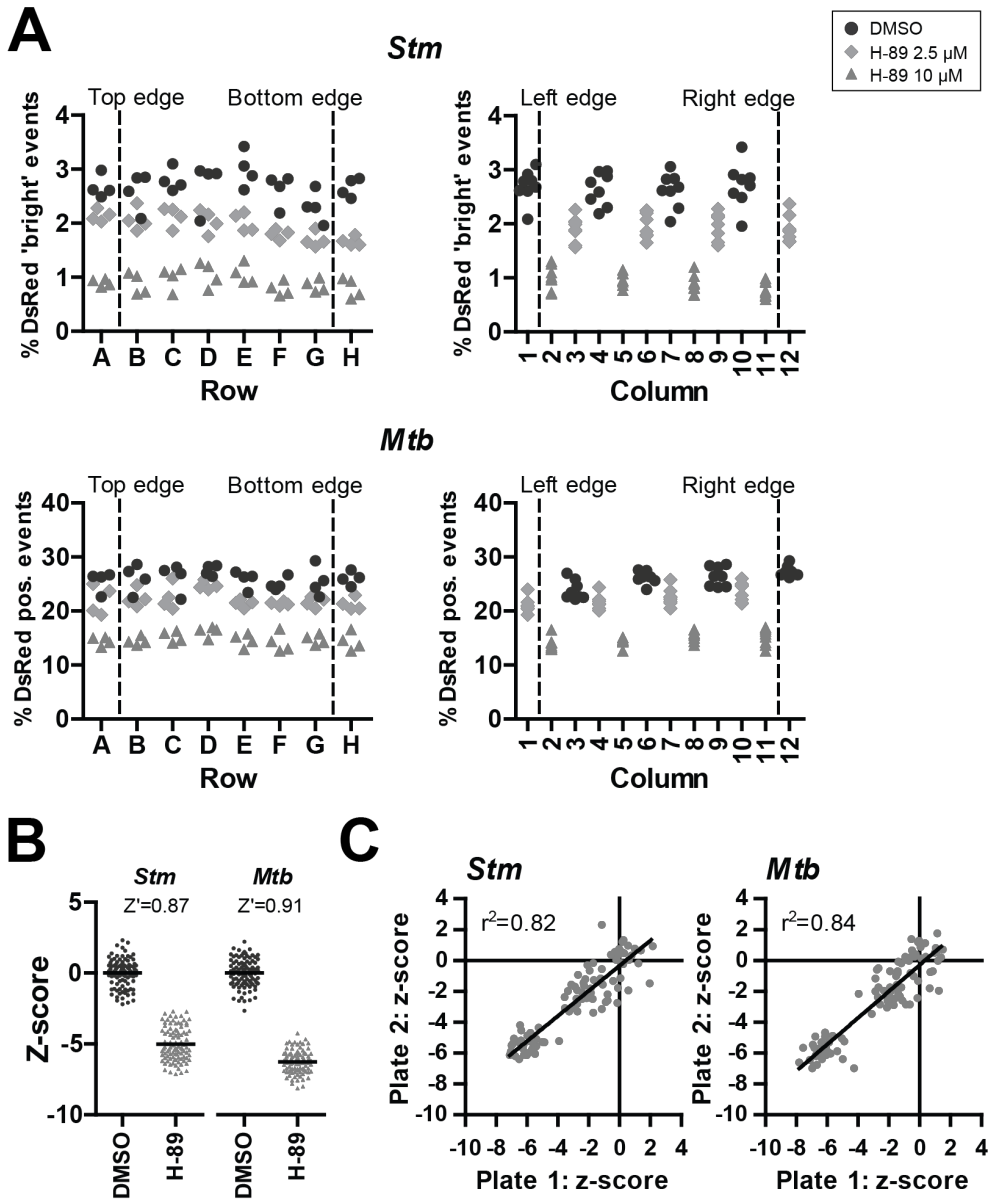
We next further optimized both the reverse siRNA transfection strategy and bacterial infection conditions by varying cell density, multiplicity of infection (MOI), infection time point and the harvesting time point for analysis using the optimal fluorescent reporters in a medium-throughput setting (96-well format). As shown in **Figure 3A**, knockdown of AKT1 was highly efficient in both HeLa and MelJuSo cells, routinely resulting in 87-97% knockdown at 72 hours post transfection. To determine an optimal infection window, knockdown kinetics were assessed until

96 hours post transfection. The largest decrease in AKT1 protein levels was observed between 48 and 72 hours post transfection, concurring with the reported 6 to 36 hour half-life of AKT1^{46,47} (**Figure 3B**). AKT1 knockdown followed identical kinetics in both HeLa and MelJuSo cells. As cell over-confluence was observed at 96 hours post transfection the assay was not extended beyond this time point. By varying both the time point of infection (24-72 hours post transfection) and the time between infection and readout (24-72 hours) within a 96 hour timeframe, we determined that the optimal assay window for *Stm* infections



↑ **Figure 3. Knockdown of AKT1 in HeLa and MelJuSo cells.**

A. Western blot showing AKT1 knockdown (siAKT1) compared to scrambled siRNA (siCTRL) in HeLa (left panel) and MelJuSo (right panel) whole cell lysates at 72 hours post transfection. β -Actin was included as loading control. **B.** Time course of AKT1 silencing by western blot analysis, normalized for β -Actin. AKT1 protein abundance is shown relative to cells transfected with scrambled siRNA between 24 to 96 hours post transfection (black line). The dotted and dashed lines represent theoretical 6 to 36-hour half-lives reported for AKT1, respectively. The horizontal bars depict the infection time windows for both *Stm* and *Mtb* used in the final screening assay.



← **Figure 4. Screening assay window, reproducibility, uniformity and validation.**

A. Plate uniformity test using HeLa cells infected with *Stm* constitutively expressing stable DsRed (top panel) or MelJuSo cells infected with *Mtb* constitutively expressing stable DsRed (bottom panel) and treated with 2.5 μ M H-89, 10 μ M H-89 or DMSO at equal v/v. The percentage of gated 'bright' (top panel) or total (bottom panel) DsRed positive events from individual wells were grouped either by row (left panel) or by column (right panel). The dashed lines

indicate the wells on the edges of the plates to identify edge effects. **B.** Assay windows for both the HeLa-*Stm* and the MelJuSo-*Mtb* infection models (as in **A**) following assay optimization. Z' factors are displayed for each infection model. Shown are 96 individual replicates of infected cells treated with 10 μ M H-89 or DMSO. Percentages of DsRed 'bright' cells (HeLa-*Stm*) and DsRed positive cells (MelJuSo-*Mtb*) are expressed as a z-score. **C.** Comparison of individual plates from plate uniformity tests for HeLa-*Stm* (left panel) and MelJuSo-*Mtb* (right panel) infection models (as in **A**). Z-scores were plotted for individual wells and a correlation coefficient was calculated by linear regression.

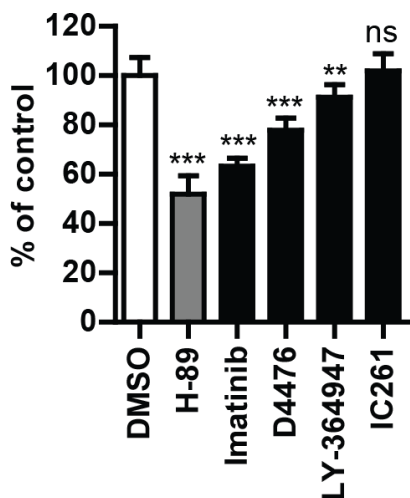
was obtained when HeLa cells were infected 72 hours post transfection followed by a 24 hour incubation until readout by flow cytometry, while *Mtb* infections resulted in the largest possible assay window when MelJuSo cells were infected 24 hours post transfection followed by a 48 hour incubation until readout by flow cytometry (**Figure 3B**).

Screening assay window, reproducibility, uniformity and validation.

To further confirm assay uniformity and reproducibility, plate uniformity assays were performed and the assay conditions were optimized according to any drift or edge effects that were observed. Results from representative 96-well plates using the optimized screening conditions for *Stm* and *Mtb* are displayed in **Figure 4A**, indicating that the assay generates highly uniform results within the assay plates. The assay yielded an assay window (expressed as a Z' factor) of 0.87 for infections with *Stm* and 0.91 for *Mtb*, greatly exceeding the minimal acceptable Z' factor of 0.4 (**Figure 4B**). In addition, inter-plate reproducibility was high for both infection models ($r^2 = 0.82$ for *Stm* infections and $r^2 = 0.84$ for *Mtb* infections) (**Figure 4C**).

Validation of the MelJuSo-*Mtb* model and the novel screening assay

To validate the MelJuSo model system, we tested already published host-directed compounds with known activity against *Mtb* here in this model; indeed, as expected these known compounds also reduced *Mtb* loads in MelJuSo cells and in human M ϕ s upon short (overnight) treatment (at standard 10 μ M concentrations). As shown in **Figure 5**, Imatinib, D4476, and LY-364947 all decreased the *Mtb* bacterial load in our model, well in agreement with previous studies^{23,26}. In addition, we also confirmed that a dual inhibitor of TGFbetaR1 and Casein Kinase 1 (D4476) inhibited *Mtb* more potently than the individual inhibitors of TGFbetaR1 (LY-364947) and Casein Kinase 1 (IC261) alone, confirming data from Jayaswal *et al.*²³ (**Figure 5**). Finally, during the work described in this thesis also Haloperidol²⁴ was confirmed to inhibit both *Stm* and *Mtb* in our model and these results will be discussed in more detail in **Chapter 3**. Thus, the results obtained in our novel MelJuSo-*Mtb* infection model and flow cytometry-based readout of intracellular infection faithfully reproduce the reported inhibitory effects of previously published compounds, providing important biological plausibility for



← **Figure 5. Verification of host-directed *Mtb* inhibitors from literature in the novel screening assay.**

Overnight treatment of MeJJuSo cells infected with *Mtb* constitutively expressing stable DsRed with compounds that were previously reported to be active against *Mtb* at 10 μ M or with DMSO at equal v/v. H-89 is used as a positive control at 10 μ M²¹. The *Mtb* bacterial load is displayed as a percentage of the DMSO control +/- standard deviation to indicate the extent of bacterial inhibition. Statistically significant difference compared to DMSO was tested using a one-way ANOVA. (ns = not significant, ** = p-value < 0.01, *** = p-value < 0.001).

the system. Of note, none of the published compounds evaluated above was more potent in inhibiting intracellular *Mtb* than our reference compound H-89. We therefore used our assay to screen chemical libraries to identify host-directed inhibitors with more potent activity than H-89 in **Chapters 3 and 4**.

Discussion

Here, we report the development and validation of a novel fluorescence-based screening assay that is able to rapidly quantify intracellular bacterial infection in human cells, as described here we think is important since it helps shortening the readout from a classical 3-week CFU assay for *Mtb* to 24-72h using flow cytometry. The assay is highly reproducible, medium-throughput, provides an excellent assay window, and is suitable for screening both chemical compound and siRNA libraries. Taking advantage of the previously reported phagocytic capability of melanocytes³⁹, we also report the human melanoma cell line MeJJuSo as a novel model for *Mtb* infection studies, particularly for studies encompassing chemical and RNAi screens. This model has considerable potential to facilitate advanced research into host-directed therapies in TB for several reasons. Firstly, due to their clonal origin cell lines are substantially more homogeneous than primary cells from different donors. This greatly enhances reproducibility and enables substantial upscaling of the assay. Secondly, MeJJuSo cells do not require any additional stimulation in contrast to the often-used THP-1 infection model, avoiding skewing of cell signaling prior to experimental stimuli. Thirdly, MeJJuSo cells are highly manipulable by siRNA and their transfectability enables studying intracellular *Mtb* in cell lines overexpressing a gene of interest or expressing fluorescently tagged proteins. Each of these properties render MeJJuSo cells ideally suitable for the high-content screening stages of host-directed chemical

genetics research, which can then be followed by validation of a limited selection of hits in human primary Mφs. Importantly, our assay faithfully reproduces the inhibitory effect of several previously published host-directed compounds (that were identified using different strategies, approaches and models) on *Mtb* intracellular survival as well as HDT results obtained in human primary Mφs, further validating our novel infection model.

High stability of reporter proteins can pose major problems in fluorescent assays for bacteria viability, especially in case of slowly proliferating bacteria like *Mtb*. In our experiments chemical compound treatment induced a robust phenotype resulting in strong changes in the fluorescent signal when using stable fluorescent proteins such as DsRed. In contrast, siRNA induced more subtle phenotypes, likely due to relatively specific gene targeting, protein stability and potential target redundancy. In this case decreased bacterial viability resulting from host gene knockdown may be masked by residual stable fluorescence. Importantly, we here showed that conditional or destabilized DsRed constructs for (myco)bacterial expression can aid in overcoming this problem, by sufficiently increasing the assay sensitivity for host-directed siRNA screens. In our experiments, both the reference compound H-89 and AKT1 silencing were unable to induce complete host-mediated *Mtb* inhibition. Considering that none of the compounds displayed in **Figure 5** surpassed the *Mtb* inhibitory potency of H-89, more and substantially better chemical compounds and drugable targets must be identified to firmly establish host-directed therapy as a feasible option for complementary treatment of TB. To this end, we employed the screening assay reported here for chemical compound screens of up to 1,200 compounds and siRNA screens of up to 1,000 siRNA pools (results in **Chapters 3** and **4**), yielding highly reproducible results with a good signal window and identifying chemical compounds and siRNA pools that perform considerably better than H-89 and AKT1 silencing, respectively. Importantly, top hit compounds from these screens were subsequently successfully validated in human primary Mφs.

The advent of high-throughput screens for host-directed intervention in intracellular bacterial infections gave rise to several different screening efforts employing methods ranging from traditional CFU assays^{22,23} to bioluminescent assays^{48,49} and automated microscopy^{24,50} all with their individual merits and pitfalls. Despite being the golden standard in TB research, CFU assays are not ideally suitable for high-throughput screens due to their laborious nature and the slow proliferation of *Mtb*. Additionally, individual *Mtb* colonies are often hard to distinguish due to their irregular morphology and variable size, adding to the inaccuracy of the assay. As an alternative to CFU assays, efforts have been made to optimize bioluminescent constructs for expression in mycobacteria⁴⁸ and to develop bioluminescent screening assays⁴⁹. Though reliable and rapid, bioluminescent assays are severely limited when compared to flow cytometry or microscopy based readouts, due to their single-parameter measurement at the well level rather than at the (sub)cellular or population levels. In contrast, phenotypic screens using automated microscopy can be tremendously informative but automated microscopy platforms require a major investment and analysis is often dependent on proprietary image analysis software. The computational infrastructure for the complex analyses and storage of the

excessive quantities of data generated using this method in a high-content setting are not currently in place in many laboratories. Our novel flow cytometry-based screening assay bridges the gap between the methods outlined above, combining the simplicity, ease of use and straightforward analysis of bioluminescent assays with the multiparametric readout, versatility and high quantifiability of fluorescence microscopy.

Experimental procedures

Reagents

H-89 dihydrochloride, D4476, IC261, LY-364947, Rifampicin and Kanamycin were purchased from Sigma-Aldrich, Zwijndrecht, The Netherlands. Hygromycin B was acquired from Life Technologies-Invitrogen, Bleiswijk, The Netherlands. Imatinib mesylate was from Enzo Life Sciences, Raamsdonksveer, The Netherlands. Ampicillin was purchased from Calbiochem Merck-Millipore, Darmstadt, Germany.

Cell culture

HeLa cells and the MelJuSo human melanoma cell line were maintained at 37°C and 5% CO₂ in Gibco Iscove's Modified Dulbecco's Medium (IMDM; Life Technologies-Invitrogen) with 10% fetal bovine serum (FBS, Greiner Bio-One, Alphen a/d Rijn, The Netherlands), 100 units/ml Penicillin and 100 µg/ml Streptomycin (Life Technologies-Invitrogen). Pro-inflammatory Mφ1s and anti-inflammatory Mφ2s were generated from monocytes isolated from whole blood of healthy donors by FICOLL separation and CD14 MACS sorting (Miltenyi Biotec, Teterow, Germany) followed by 6 days differentiation with 5 ng/ml granulocyte macrophage-colony stimulating factor (GM-CSF; BioSource Life Technologies-Invitrogen) or 50 ng/ml macrophage-colony stimulating factor (M-CSF; R&D Systems, Abingdon, United Kingdom) respectively, as previously reported⁵¹. Mφs were cultured in Gibco Roswell Park Memorial Institute (RPMI) 1640 medium (Life Technologies-Invitrogen) with 10% FBS and 2 mM L-Alanyl-L-Glutamine (PAA, Linz, Austria).

Bacterial culture

Bacterial strains used are displayed in **Table 1**. Mycobacteria were cultured in Difco Middlebrook 7H9 broth (Becton Dickinson, Breda, The Netherlands) supplemented with 10% ADC (Becton Dickinson), 0.5% Tween-80 (Sigma-Aldrich) and appropriate antibiotics. *Stm* was cultured on Difco Luria-Bertani (LB) agar (Becton Dickinson) or in Difco LB broth (Becton Dickinson) supplemented with appropriate antibiotics.

Stm and *Mtb* infections

One day before infection, mycobacterial cultures were diluted to a density corresponding with early log phase growth (optical density at 600 nm (OD₆₀₀) of 0.4). *Stm* was grown either in LB broth or on LB agar with appropriate antibiotics. After overnight incubation *Stm* liquid cultures were diluted 1:33 and cultured for an

Table 1. Bacterial strains, plasmids used for fluorescent protein expression and their respective antibiotic selection markers.

Base strain	Plasmid	Antibiotic resistance (source, concentration)
<i>Stm</i> SL1344.	pMW211[C.10E/DsRed] (Constitutive promoter).	Ampicillin (plasmid, 100 µg/ml).
<i>Stm</i> SL1344.	pMW215[PpagC/DsRed] (Low-pH inducible promoter).	Ampicillin (plasmid, 100 µg/ml).
<i>Stm</i> SL1344.	pMW266[PpagC/destabilized DsRed] (Low-pH inducible promoter).	Ampicillin (plasmid, 100 µg/ml).
<i>Mtb</i> H37Rv.	pSMT3[Phsp60/DsRed].	Hygromycin (plasmid, 50 µg/ml).
<i>Mtb</i> H37Rv.	pSMT3[Phsp60/GFP].	Hygromycin (plasmid, 50 µg/ml).
<i>Mtb</i> H37Rv.	pSMT3[Phsp60/destabilized DsRed].	Hygromycin (plasmid, 50 µg/ml).

additional 3-4 hours while plate grown *Stm* was suspended in PBS by rinsing the agar plates. Bacterial density was determined by measuring the OD₆₀₀ and the bacterial suspension was diluted in cell culture medium without antibiotics to reach a multiplicity of infection (MOI) of 10 (unless indicated otherwise). Accuracy of bacterial density measurements was verified by a standard colony forming unit (CFU) assay. Cell cultures (HeLa for *Stm* infections and MelJuSo for *Mtb* infections), seeded in 96-well flat-bottom plates as described below, were inoculated with 100 µl of the bacterial suspension, centrifuged for 3 minutes at 800 rpm and incubated at 37°C/5% CO₂ for 20 minutes if infected with *Stm* or 60 minutes if infected with *Mtb*. Plates were then washed with culture medium containing 30 µg/ml gentamicin sulfate (Lonza BioWhittaker, Basel, Switzerland) and incubated at 37°C and 5% CO₂ in medium containing 5 µg/ml gentamicin and indicated chemical compounds until readout by flow cytometry or CFU, as indicated.

Chemical compound treatment

10,000 HeLa or MelJuSo cells were seeded per well in 96-well flat-bottom plates or 300,000 primary Mφs were seeded per well in 24-well plates in appropriate culture medium without antibiotics one day prior to infection with *Mtb* or broth-grown *Stm*. Infected cells were treated overnight with chemical compounds at 10 µM (unless indicated otherwise) or DMSO at equal v/v in medium containing 5 µg/ml gentamicin.

siRNA transfections

3,000 HeLa or MelJuSo cells were reverse-transfected with ON-TARGETplus siRNA pools (Thermo Fisher Dharmacon, Waltham Massachusetts, USA) at a 50 nM concentration using 0.2 µl Dharmafect1 (Thermo Fisher Dharmacon) per well in

a flat-bottom 96-well plate in appropriate culture medium without antibiotics. Knockdown efficiency was verified by immunoblotting at indicated time points. Cells transfected with siRNA were infected with *Mtb* at MOI 1000 24 hours post transfection and incubated for an additional 48 hours and infections with agar-grown *Stm* were carried out at MOI 500 72 hours post transfection and incubated overnight, unless indicated otherwise.

Colony forming unit assay

CFU assays were performed using the track dilution method described previously⁵². In short, bacterial suspensions were serially diluted and 10 μ l drops were plated on square agar plates, which were subsequently placed at an angle to allow the drops to spread over a larger surface area.

Generation of a mycobacterial destabilized DsRed construct and expression in *Mtb* H37Rv

The destabilized DsRed gene (DsRed C-terminally fused to amino acids 422-461 of the mouse ornithine decarboxylase (MODC) to induce ubiquitin-independent proteasomal degradation³⁰) was amplified from the pMW266[PpagC/destabilized DsRed] plasmid by PCR and cloned into the Gateway (Invitrogen) adapted mycobacterial expression plasmid pSMT3³¹. In this vector, expression of destabilized DsRed is constitutive and controlled by the hsp60 promoter. Electrocompetent *Mtb* H37Rv were freshly prepared from a 100 ml log-phase culture by incubation at 4°C for 90 minutes followed by suspension of the bacteria in 1 ml ice cold PBS containing 10% glycerol. 100 μ l Bacterial suspension was then transformed with 1 μ g plasmid DNA by electroporation. Transformed bacteria were suspended in 10 ml 7H9 broth, incubated overnight at 37°C and subsequently plated on Difco Middlebrook 7H10 agar (Becton Dickinson, Breda, The Netherlands) under Hygromycin (50 μ g/ml) selection (Life Technologies-Invitrogen, Bleiswijk, The Netherlands). DsRed expression of individual clones was verified by flow cytometry.

Fluorescence microscopy

100,000 HeLa or MeJuSo cells were grown on glass coverslips (Menzel-Gläser, Braunschweig, Germany) in 24-well plates and infected as described above. Samples were fixed for 30 minutes at RT with 4% paraformaldehyde, embedded in VectaShield with DAPI (Brunschiwig Chemie, Amsterdam, The Netherlands) and examined on an Axioskop 2 fluorescence microscope (Carl Zeiss, Sliedrecht, The Netherlands).

Screening assay validation and screening statistics

The flow cytometry-based screening assay for *Stm* and *Mtb* infection of human cell lines was developed adhering to guidelines published by the NIH Chemical Genomics Center⁵³. Cells were transfected and infected with *Stm* or *Mtb* in flat-bottom 96-wells plates as described above. Cells were harvested by trypsinization and fixed with 1% paraformaldehyde prior to readout using a FACSCalibur (Becton Dickinson) with high-throughput sampler (HTS) extension (Becton

Dickinson). Data was analyzed using FlowJo for Mac OS X version 8.8.7 (TreeStar, Ashland, OR, USA) and both the total and bright DsRed positive populations expressed as a frequency of the parent forward/side-scatter gate and the total event counts were extracted for further analysis. Z' factors (to determine the assay window) were calculated using the formula $Z' = \frac{(AVG_{DMSO} - \frac{3SD_{DMSO}}{\sqrt{n}}) - (AVG_{H-89} + \frac{3SD_{H-89}}{\sqrt{n}})}{AVG_{DMSO} - AVG_{H-89}}$, where AVG is the average percentage of DsRed positive events measured after DMSO or H-89 treatment, SD is the standard deviation of these measurements and n is the number of replicates. Z-scores were calculated using the formula $z = \frac{x - AVG_{DMSO}}{STDEV_{DMSO}}$ where the difference between the percentage of DsRed positive events (bacterial load) or the total event count (cell viability) of a single replicate of an experimental condition (x) and the average percentage of DsRed positive events or the total event count of the DMSO control (AVG_{DMSO}) is divided by the standard deviation of the DMSO control (STDEV_{DMSO}). An average z-score ≤ -2 or ≥ 2 was used as a hit cut-off, unless otherwise indicated.

Immunoblotting

Cells were lysed by heating in loading buffer (250 mM Tris, 8% w/v SDS, 20% glycerol, 20% β -mercaptoethanol and 0.002% w/v bromophenolblue) for 5 minutes at 99°C. Proteins from lysates of 50,000 cells were mass-separated by SDS-PAGE gel electrophoresis and subsequently blotted on a PVDF membrane. Following fixation in pure methanol for 15 seconds at RT, membranes were blocked for 1 hour at RT with 5% w/v milk. Blots were then incubated overnight at 4°C with mouse anti-human AKT1 IgG1 (1:5,000; Cell Signaling Technology, Leiden, The Netherlands) diluted in 5% w/v milk. After incubation, membranes were washed for 1 hour at RT with PBS containing 0.1% Tween-20, refreshing the wash buffer every 10 minutes. Blots were incubated with HRP-labelled goat anti-mouse IgG (1:12,500; Thermo Scientific, Bleiswijk, The Netherlands) and HRP-labelled goat anti-human actin (1:80,000; Santa Cruz, Heidelberg, Germany) diluted in 5% w/v milk for 1 hour at RT and washed as above. Protein bands were visualized on a photosensitive film by Enhanced ChemiLuminescence (ECL Plus, Amersham-GE Healthcare, Freiburg, Germany). Relative protein abundance was quantified by calculating the area under the curve (AUC) for each band using ImageJ (version 1.43n) and each lane was normalized against the AUC of the actin band.

Statistics

Student's T-test, one-way ANOVA and linear regression were performed using GraphPad Prism version 6.0 for Mac OS X (GraphPad Software, San Diego California, USA; www.graphpad.com).

References

1. Barry, C. E. & Blanchard, J. S. The chemical biology of new drugs in the development for tuberculosis. *Curr Opin Chem Biol* **14**, 456–466 (2010).

2. Norrby, S. R., Nord, C. E., Finch, R. European Society of Clinical Microbiology and Infectious Diseases. Lack of development of new antimicrobial drugs: a potential serious threat to public health. *Lancet Infect Dis* **5**, 115–119 (2005).
3. Becker, D. *et al.* Robust Salmonella metabolism limits possibilities for new antimicrobials. **440**, 303–307 (2006).
4. Makarov, V. *et al.* Benzothiazinones kill Mycobacterium tuberculosis by blocking arabinan synthesis. *Science* **324**, 801–804 (2009).
5. Christophe, T. *et al.* High content screening identifies decaprenyl-phosphoribose 2' epimerase as a target for intracellular antimycobacterial inhibitors. *PLoS Pathog* **5**, e1000645 (2009).
6. Willand, N. *et al.* Synthetic EthR inhibitors boost antituberculous activity of ethionamide. *Nat. Med.* **15**, 537–544 (2009).
7. Lawn, S. D. & Zumla, A. I. Tuberculosis. *Lancet* **378**, 57–72 (2011).
8. Ottenhoff, T. H. M. New pathways of protective and pathological host defense to mycobacteria. *Trends Microbiol.* **20**, 419–428 (2012).
9. Santos, R. L. *et al.* Animal models of Salmonella infections: enteritis versus typhoid fever. *Microbes Infect.* **3**, 1335–1344 (2001).
10. Guiney, D. G. & Lesnick, M. Targeting of the actin cytoskeleton during infection by Salmonella strains. *Clin. Immunol.* **114**, 248–255 (2005).
11. Holden, D. W. Trafficking of the Salmonella vacuole in macrophages. *Traffic* **3**, 161–169 (2002).
12. Brumell, J. H. & Grinstein, S. Salmonella redirects phagosomal maturation. *Current Opinion in Microbiology* **7**, 78–84 (2004).
13. Kaufmann, S. H. How can immunology contribute to the control of tuberculosis? *Nat Rev Immunol* **1**, 20–30 (2001).
14. Vergne, I., Chua, J., Singh, S. B. & Deretic, V. Cell biology of mycobacterium tuberculosis phagosome. *Annu. Rev. Cell Dev. Biol.* **20**, 367–394 (2004).
15. Cooper, A. M. Cell-mediated immune responses in tuberculosis. *Annu. Rev. Immunol.* **27**, 393–422 (2009).
16. Diedrich, C. R. & Flynn, J. L. HIV-1/mycobacterium tuberculosis coinfection immunology: how does HIV-1 exacerbate tuberculosis? *Infection and Immunity* **79**, 1407–1417 (2011).
17. Ottenhoff, T. H. M. The knowns and unknowns of the immunopathogenesis of tuberculosis. *Int. J. Tuberc. Lung Dis.* **16**, 1424–1432 (2012).
18. World Health Organization. *Global tuberculosis report 2015.* (2015).
19. Ottenhoff, T. H. M. Overcoming the global crisis: ‘yes, we can’, but also for TB ... ? *Eur. J. Immunol.* **39**, 2014–2020 (2009).
20. Jassal, M. S. & Bishai, W. R. Epidemiology and challenges to the elimination of global tuberculosis. *CLIN INFECT DIS* **50 Suppl 3**, S156–64 (2010).
21. Kuijl, C. *et al.* Intracellular bacterial growth is controlled by a kinase network around PKB/AKT1. **450**, 725–730 (2007).
22. Kumar, D. *et al.* Genome-wide analysis of the host intracellular network that regulates survival of Mycobacterium tuberculosis. *Cell* **140**, 731–743 (2010).

23. Jayaswal, S. *et al.* Identification of host-dependent survival factors for intracellular *Mycobacterium tuberculosis* through an siRNA screen. *PLoS Pathog* **6**, e1000839 (2010).
24. Sundaramurthy, V. *et al.* Integration of chemical and RNAi multiparametric profiles identifies triggers of intracellular mycobacterial killing. *Cell Host and Microbe* **13**, 129–142 (2013).
25. Machado, D. *et al.* Ion Channel Blockers as Antimicrobial Agents, Efflux Inhibitors, and Enhancers of Macrophage Killing Activity against Drug Resistant *Mycobacterium tuberculosis*. *PLoS ONE* **11**, e0149326 (2016).
26. Napier, R. J. *et al.* Imatinib-sensitive tyrosine kinases regulate mycobacterial pathogenesis and represent therapeutic targets against tuberculosis. *Cell Host and Microbe* **10**, 475–485 (2011).
27. Subbian, S. *et al.* Phosphodiesterase-4 inhibition alters gene expression and improves isoniazid-mediated clearance of *Mycobacterium tuberculosis* in rabbit lungs. *PLoS Pathog* **7**, e1002262 (2011).
28. Subbian, S. *et al.* Phosphodiesterase-4 inhibition combined with isoniazid treatment of rabbits with pulmonary tuberculosis reduces macrophage activation and lung pathology. *Am. J. Pathol.* **179**, 289–301 (2011).
29. Koo, M.-S. *et al.* Phosphodiesterase 4 inhibition reduces innate immunity and improves isoniazid clearance of *Mycobacterium tuberculosis* in the lungs of infected mice. *PLoS ONE* **6**, e17091 (2011).
30. Vilaplana, C. *et al.* Ibuprofen therapy resulted in significantly decreased tissue bacillary loads and increased survival in a new murine experimental model of active tuberculosis. *Journal of Infectious Diseases* **208**, 199–202 (2013).
31. Mayer-Barber, K. D. *et al.* Host-directed therapy of tuberculosis based on interleukin-1 and type I interferon crosstalk. **511**, 99–103 (2014).
32. Datta, M. *et al.* Anti-vascular endothelial growth factor treatment normalizes tuberculosis granuloma vasculature and improves small molecule delivery. *Proc Natl Acad Sci USA* **112**, 1827–1832 (2015).
33. Oehlers, S. H. *et al.* Interception of host angiogenic signalling limits mycobacterial growth. **517**, 612–615 (2015).
34. Schiebler, M. *et al.* Functional drug screening reveals anticonvulsants as enhancers of mTOR-independent autophagic killing of *Mycobacterium tuberculosis* through inositol depletion. *EMBO Molecular Medicine* **7**, 127–139 (2015).
35. Skerry, C. *et al.* Simvastatin increases the in vivo activity of the first-line tuberculosis regimen. *J. Antimicrob. Chemother.* **69**, 2453–2457 (2014).
36. Stanley, S. A. *et al.* Identification of host-targeted small molecules that restrict intracellular *Mycobacterium tuberculosis* growth. *PLoS Pathog* **10**, e1003946 (2014).
37. Liu, W. S. & Heckman, C. A. The sevenfold way of PKC regulation. *Cell. Signal.* **10**, 529–542 (1998).
38. Wu-zhang, A. X. & Newton, A. C. Protein kinase C pharmacology: refining the toolbox. *Biochem. J.* **452**, 195–209 (2013).
39. Le Poole, I. C. *et al.* Phagocytosis by normal human melanocytes in vitro. *Exp. Cell Res.* **205**, 388–395 (1993).

40. Le Poole, I. C. *et al.* A novel, antigen-presenting function of melanocytes and its possible relationship to hypopigmentary disorders. *J. Immunol.* **151**, 7284–7292 (1993).
41. van Ham, S. M. *et al.* HLA-DO is a negative modulator of HLA-DM-mediated MHC class II peptide loading. *Curr. Biol.* **7**, 950–957 (1997).
42. van Ham, M. *et al.* Modulation of the major histocompatibility complex class II-associated peptide repertoire by human histocompatibility leukocyte antigen (HLA)-DO. *J. Exp. Med.* **191**, 1127–1136 (2000).
43. Martínez-Lorenzo, M. J., Méresse, S., de Chastellier, C. & Gorvel, J. P. Unusual intracellular trafficking of *Salmonella typhimurium* in human melanoma cells. *Cellular Microbiology* **3**, 407–416 (2001).
44. Verkhusha, V. V. *et al.* High stability of Discosoma DsRed as compared to Aequorea EGFP. *Biochemistry* **42**, 7879–7884 (2003).
45. Li, X. *et al.* Generation of destabilized green fluorescent protein as a transcription reporter. *J. Biol. Chem.* **273**, 34970–34975 (1998).
46. Basso, A. D. *et al.* Akt forms an intracellular complex with heat shock protein 90 (Hsp90) and Cdc37 and is destabilized by inhibitors of Hsp90 function. *J. Biol. Chem.* **277**, 39858–39866 (2002).
47. Liao, Y. *et al.* Peptidyl-prolyl cis/trans isomerase Pin1 is critical for the regulation of PKB/Akt stability and activation phosphorylation. *Oncogene* **28**, 2436–2445 (2009).
48. Andreu, N. *et al.* Optimisation of bioluminescent reporters for use with mycobacteria. *PLoS ONE* **5**, e10777 (2010).
49. Eklund, D. *et al.* Validation of a medium-throughput method for evaluation of intracellular growth of *Mycobacterium tuberculosis*. *Clin. Vaccine Immunol.* **17**, 513–517 (2010).
50. Brodin, P. *et al.* High content phenotypic cell-based visual screen identifies *Mycobacterium tuberculosis* acyltrehalose-containing glycolipids involved in phagosome remodeling. *PLoS Pathog* **6**, e1001100 (2010).
51. Verreck, F. A. W., de Boer, T., Langenberg, D. M. L., van der Zanden, L. & Ottenhoff, T. H. M. Phenotypic and functional profiling of human proinflammatory type-1 and anti-inflammatory type-2 macrophages in response to microbial antigens and IFN-gamma- and CD40L-mediated costimulation. *Journal of Leukocyte Biology* **79**, 285–293 (2006).
52. Jett, B. D., Hatter, K. L., Huycke, M. M. & Gilmore, M. S. Simplified agar plate method for quantifying viable bacteria. *BioTechniques* **23**, 648–650 (1997).
53. Singhal, A. *et al.* Metformin as adjunct antituberculosis therapy. *Science Translational Medicine* **6**, 263ra159–263ra159 (2014).